Buckling Behavior of Single Layer Grid Shell Using Newly Developed Light Weight Rigid Joint

Dr. Masumi FUJIMOTO*, Prof. Katsuhiko IMAI**,
Mr. Ryoji KINOSHITA*** and Mr. Tokio MORITA***
* Faculty of Engineering, Osaka City University,
Sugimoto, Sumiyoshiku, Osaka 558-8585, Japan
Tel int+81-6-605-2989, Fax int+81-6-605-2989
e-mail address: fujimoto@arch.eng.osaka-cu.ac.jp
** The Graduate School of Engineering.,
Dep. of Global Architecture, Osaka University,
Yamadaoka, Suita, Osaka 565-0871, Japan
Tel int+81-6-879-7566, Fax int+81-6-879-7566
e-mail address: karl@ga.eng.osaka-u.ac.jp
*** Kawasaki Steel Metal Products & Engineering Inc.
Uozakiminamimachi 3-6-24, Higashinadaku,
Kobe 658-0025, Japan
Tel int+81-78-431-4161, Fax int+81-78-431-4166

Abstract

This paper introduces a new rigid joint system of standardized truss system. This joint system is regarded as nearly rigid and is used as the joint of single layer grid shell.

In this study, the mechanical properties of this new rigid joint are obtained by bending experiment of joint subjected to axial forces. The effectiveness of this joint system is verified by numerical calculation of buckling behavior of single layer grid shells under gravity load.

The configurations of grid shells in this study are made by Formian. The steel circular hollow tube and PC bar are used as constituent members of these shells. PC bar is capable of increasing the stiffness and strength of the structure. The effect of PC bar on the buckling behavior of grid shell is also examined.

1. Introduction

In recent years, the standardized truss system joint was researched the mechanical behavior, i.e. stiffness and strength, in detail. The numerical model of joint was proposed and the validity of the model was discussed [1][2][3]. On the other hand, in case of the application of the standardized truss system to single layer grid shell, a two-way grid shell has a superior in the configuration generation and the material efficiency property to three-way grid shell. But it is demanded that the joint rigidity of two-way grid shell joint is larger than that of three-way grid shell.

In this study, the newly developed standardized truss system joint is presented in order to apply to single layer two-way grid shell. The bending experiment of joint is performed as the parameter of the size of joint and the axial force of member. The mechanical properties of this joint system are examined by experimentally. Then, the effectiveness of this joint system is verified by the numerical calculation of buckling behavior of single layer grid shells using this joint system under gravity load.

2. Experiment of New Joint System

2.1 Method of Experiment

Test specimen is composed of the node, the sleeve, the bolt of joint, the cone, the circular tube and the clevis. The configuration of specimen is shown in Fig. 1. The detail of sleeve is shown in Fig. 2. The list of specimen is shown in Table 1. Dimensions of specimen and parts are shown in Table 2. The mechanical properties of parts are shown in Table 3.

The measurement items are displacements, deformations, strains, member axial forces and the concentrated load. The specimen is pin-supported and the uniform bending moment is applied to the joint. The rotational angle of joint, θ, is used as the control parameter of experiment. The loading process is one way incremental loading.

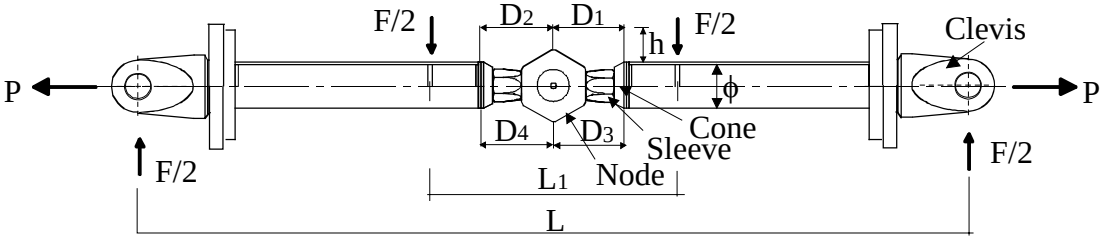

Fig. 1. Configuration of Specimen.

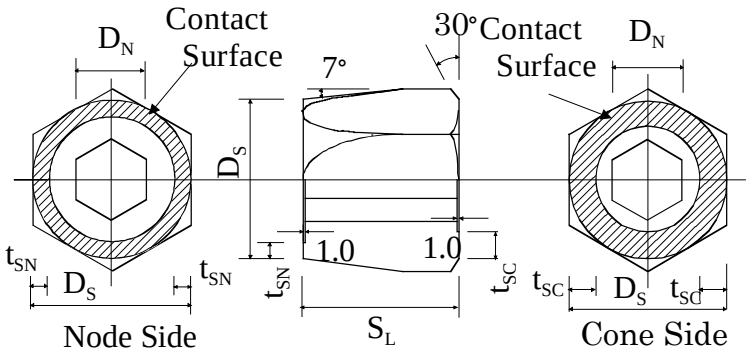

Fig. 2. Detail of Sleeve.

Table 1. List of Specimen.

Specimen	Bolt	Bolt Clamping Force	Member Axial Force
M30N0	M30	225kN	0
M36N0	M36	336kN	0
M36T20	M36	336kN	196kN
M36C40	M36	336kN	-392kN
M42N0	M42	446kN	0
M48N0	M48	593kN	0

Table 2. Dimensions of Specimen and Parts.

	M30N0	M36N0	M42N0	M48N0
L_1(mm)	720	860	1000	1140
L(mm)	2400	2400	3600	3600
Node(mm)	ϕ210/190	ϕ235/210	ϕ270/242	ϕ300/268
Diameter of Tube(mm)	ϕ139.8	ϕ165.2	ϕ190.7	ϕ216.3
Thickness of Tube(mm)	6.6	7.1	7.0	8.2
D_S(mm)	83	100	115	130
D_N(mm)	37	42.5	48	56
S_L(mm)	81	97	111	129
t_{SN}(mm)	8.5	10	12	13
t_{SC}(mm)	14	16	20	21

Table 3. Mechanical Properties of Material.

Parts	Material	Yield Stress σ_y(N/mm^2)	Tensile Strength σ_b(N/mm^2)
Bolt	SNCM439	833.	931.
Sleeve	SCM435	828.	953.
Cone	SM490	323.	498.
Node	SNCM439	787.	953.
Tube	STK400	359.	452.

2.2 Experimental Results

The relation of moment to rotational angle of joint of M36N0 is shown in Fig. 3. In which the rotational angle of joint is determined by the deformation of D_1 to D_4 in Fig. 1. This figure shows the rotational rigidity of joint directly. In this figure, the straight thick solid line shows the linear rigidity in case the specimen is composed of circular tube only.

In Fig. 4 to Fig. 7, experimental results are expressed by the envelope curve. In order to show the scale effect of joints, the relation of moment to rotational angle of specimens without member axial force is expressed in Fig. 4. To indicate the effect of member axial force, the relation of moment to rotational angle of M36 specimens is shown in Fig. 5 without the PΔ effect and in Fig. 6 with the PΔ effect respectively. The relation of moment to the strain of sleeve in lower edge of node side is shown in Fig. 7.

The initial rotational spring coefficient without the PΔ effect obtained by the moment rotational angle relation, K_1 and the bending moment corresponding to the unit deformation of loading point, K_δ are shown in Table 4. The theoretical value is obtained in condition that specimen is only composed of circular tube. For the separation moment between the sleeve and the node and that between the sleeve and the cone, the experimental result and the theoretical value are shown in Table 5. The yield moment and the maximum applied moment

of joint without the PΔ effect are shown in Table 6.

Table 4. Initial Rigidity of Joint.

Specimen	K_1(x10^5kNcm)		K_δ(x10^4kN)	
	Theory	Experiment	Theory	Experiment
M30N0	5.74	3.01	1.95	1.10
M36N0	8.23	6.07	2.46	1.90
M36T20	----	5.88	----	2.00
M36C40	----	5.20	----	1.67
M42N0	11.4	6.77	2.81	2.25
M48N0	17.3	10.0	3.68	3.16

Table 5. Separation Moment (x10^2kNcm).

Specimen	Node and Sleeve		Cone and Sleeve	
	Theory	Experiment	Theory	Experiment
M30N0	3.93	4.00	3.44	3.60
M36N0	7.09	7.00	6.28	6.05
M36T20	3.27	3.88	2.89	3.85
M36C40	14.7	15.7	13.1	10.1
M42N0	10.7	12.4	9.34	9.66
M48N0	16.3	17.9	14.4.	9.92

Table 6. Yield Moment and Maximum Applied Moment (x10^3kNcm).

Specimen	Yield Moment	Maximum Applied Moment
M30N0	1.28	1.76
M36N0	2.01	2.91
M36T20	1.57	3.51
M36C40	2.26	2.26
M42N0	3.95	4.58
M48N0	6.31	7.32

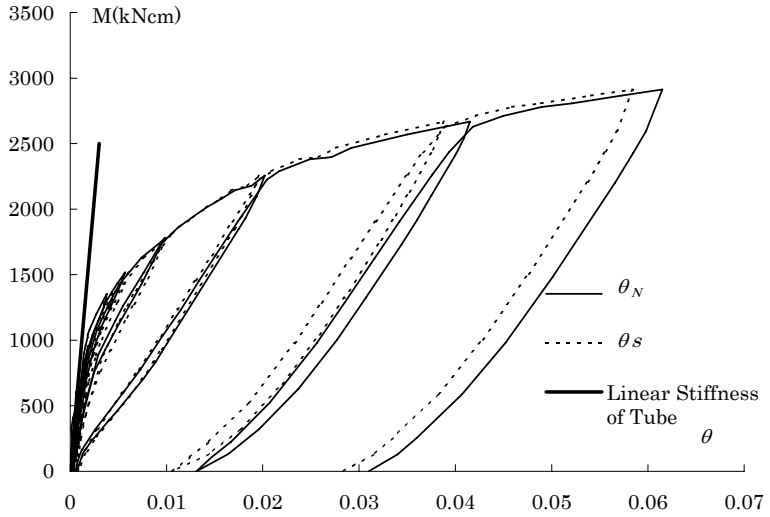

Fig. 3. Relation of Moment to Rotational Angle of Joint of M36N0.

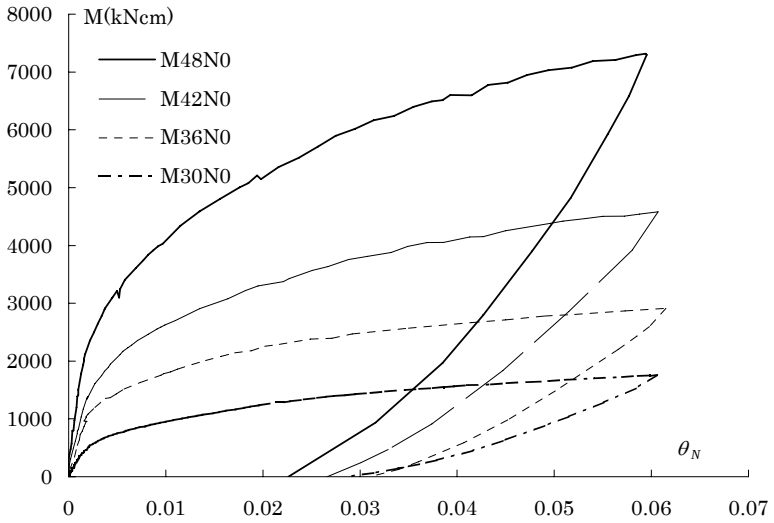

Fig. 4. Relation of Moment to Rotational Angle of Specimens without Member Axial Force.

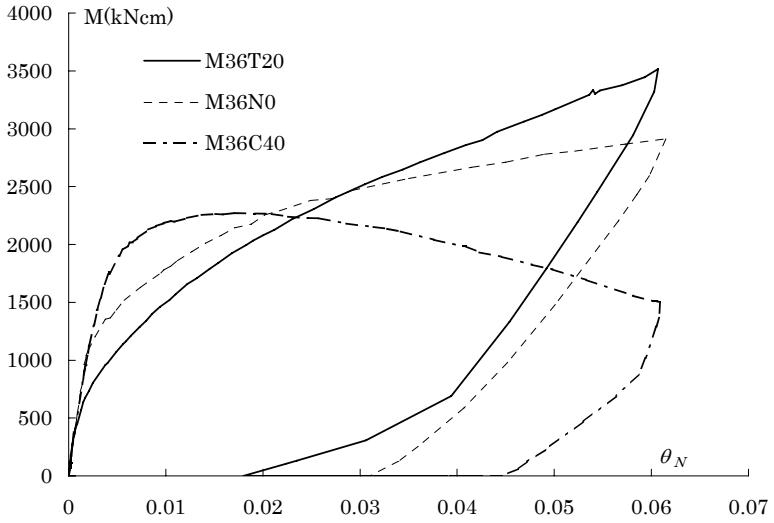

Fig. 5. Relation of Moment to Rotational Angle of M36 Specimens.

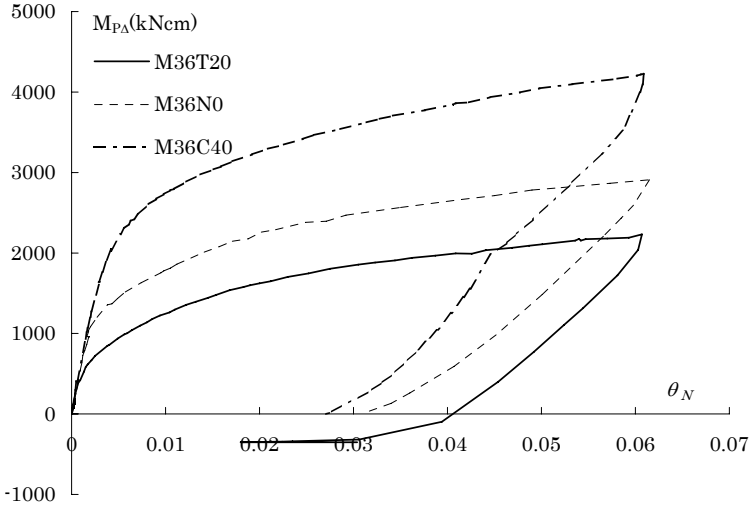

Fig. 6. Relation of PΔ Moment to Rotational Angle of M36 Specimens.

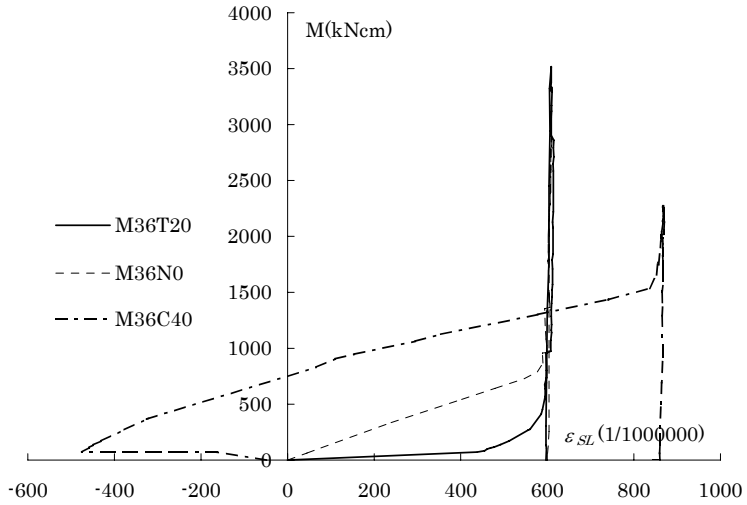

Fig. 7. Relation of Moment to Strain of Sleeve in Lower Edge of Node Side.

2.3 Considerations

2.3.1 Behavior of Deformation

As the applied load increases, the contact surface between the sleeve and the cone firstly separates at lower edge, and secondly follows between the sleeve and the node. After the separation of contact surfaces, the strain of sleeve in upper edge of node side and the average strain of bolt increase gradually. The second slope appears in the relation of moment to rotational angle. But, the load deformation relation of this joint under uniform bending moment shows almost elastic behavior in case that the rotational angle is less than 0.01.

As the load increases further, the average strain of bolt increases steadily. As a result, the third slope appears in the relation of moment to rotational angle. The relationship of moment to rotational angle of joint is almost approximated to tri-linear model.

2.3.2 Rigidity of Joint

The value of initial rotational spring coefficient without member axial force is the largest among specimens. For the rotational rigidity of joint after the separation of contact surfaces, the value without the PΔ effect decreases as member axial force changes from tension to compression. While, the values with the PΔ effect in the range of third slope are almost equal to one another without respect to member axial force.

2.3.3 Separation Moment of Joint

The Separation moment with compressive axial force is larger than without member axial force. The separation moment of contact surfaces between the sleeve and the node is larger than that of contact surfaces between the sleeve and the cone. This shows that the separation of contact surface between the sleeve and the cone precedes that between the sleeve and the node.

2.3.4 Yielding Moment of Joint

The yielding moment of joint is defined by the yielding of bolt. The yielding moment of joint as well as the separation moment of joint increases as the member axial force changes from tension to compression.

2.3.5 Comparison between Theory and Experiment

For the initial rigidity of joint, the theoretical value is obtained under the condition that specimen is only composed of circular tube. The ratio of the experimental value to the theoretical value is from 0.5 to 0.6 in case of K_1 and is from 0.5 to 0.85 in case of K_δ. This shows that the initial rigidity of joint can be predicted as 0.5 to 0.85 of the theoretical value in this study.

For the separation moment, the ratio of the experimental value to the theoretical one is from 0.7 to 1.3.

3. Numerical Calculation of Buckling Behavior of Single Layer Grid Shell

3.1 Numerical Analysis Model

The configurations of the single layer grid shell treated in this paper are generated by Formian 2 [4]. The orthogonal two-way grid plane of rectangle is projected to the spherical surface. The coordinate of center of sphere is the center of two-way grid plane and the parallel projection in vertical direction is used. Two kinds of mesh are used. One is two-way grid, Mesh G and the other is two-way grid with diagonal member, Mesh T. In this study, the two-way grid unit is 2x2 m square and the original plane is 40x20 m rectangle. The radius of sphere is 30 m. Overall configurations are shown in Fig. 8.

The Circular hollow tube is used as orthogonal two-way grid member and diagonal member. To increase the strength and stiffness of orthogonal two-way grid shell, PC bars are also used as diagonal member and are valid under tensile axial force. The initial axial force, 2 kN, is introduced to the PC bar. The member sectional properties are shown in Table 7. The newly developed light weight rigid joint is compared with the perfect rigid joint. The material properties of member and joint are shown in Table 8 and Table 9 respectively.

Two kinds of boundary condition of grid shell are adopted. One is that peripheral nodes in only X direction are pin-supported and the other is that peripheral nodes in only Y direction are pin-supported. The applied load is uniformly distributed snow load and acts on the node as the equivalent nodal concentrated load.

To indicate the efficiency of new rigid joint and the effect of PC bars, eight grid shells are adopted corresponding to the combinations of joint system, mesh pattern, diagonal member and boundary condition. The combination of parameters is shown in Table 10. The last capital of notation denoting model means the direction that peripheral nodes are pin-supported.

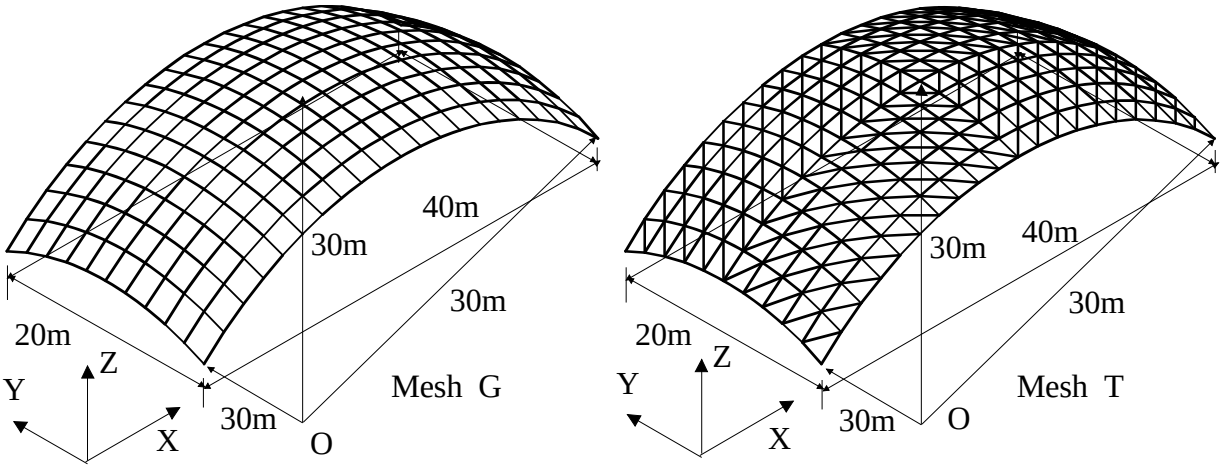

Fig. 8. Configuration of Single Layer Grid Shell.

Table 7. Member Sectional Properties.

	ϕ(mm)	A(cm^2)	Z_P(cm^3)	I(cm^4)
Circular Hollow Tube	190.7	40.4	236	1710
PC bar	13.0	1.33	0.366	0.140

Table 8. Material Properties of Member.

	Circular Hollow Tube	PC bar

Elastic Modulus (kN/cm^2)	2.08x10^4	2.08x10^4
Yield Stress (kN/cm^2)	42.0	106.

Table 9. Joint Size and Joint Material Properties.

Node	ϕ270/242
Rotational Spring Coef. (kNcm/rad)	6.77x10^5
Yield Moment(kNcm)	3.95x10^3

Table 10. Combination of Parameters.

Model	Mesh Pattern	Joint System	Diagonal Member
Type1X/ Type1Y	Mesh G	New Rigid Joint	–––––
Type2X/ Type2Y	Mesh G	Perfect Rigid Joint	–––––
Type3X/ Type3Y	Mesh T	New Rigid Joint	Circular Hollow Tube
Type4X/ Type4Y	Mesh T	New Rigid Joint	PC bar

3.2 Numerical Analysis Method

The numerical method used in this paper has been presented in previous paper [5]. A characteristic of the method is shown as follows. To consider both the size and rigidity of joint, spherical nodes and tubular member ends are modeled as rigid zone and rotational spring respectively. For PC bar member, both ends of bar are pin-jointed and the material nonliearity in tensile and compressive range is considered. To trace the equilibrium path, the arc length method is used. The subspace iteration method is adopted to calculate the buckling mode.

3.3 Numerical Results

The buckling loads of single layer grid shell under nodal gravity load are shown in Table 11. The buckling modes of representative models are shown from Fig. 9 to Fig. 12 and the axial stress distributions corresponding to the buckling load are shown in Fig. 13 to Fig. 16.

Table 11. Buckling Load.

Model	Nodal Load(kN)	Model	Nodal Load(kN)
Type1X	34.6	Type1Y	7.78
Type2X	61.3	Type2Y	15.1
Type3X	86.3	Type3Y	47.2
Type4X	53.7	Type4Y	8.88

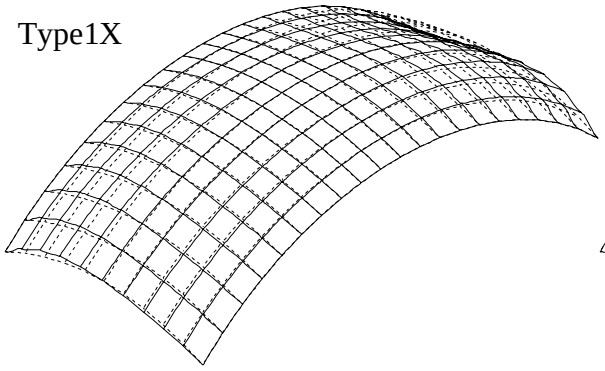

Fig. 9. Buckling Mode of Type1X.

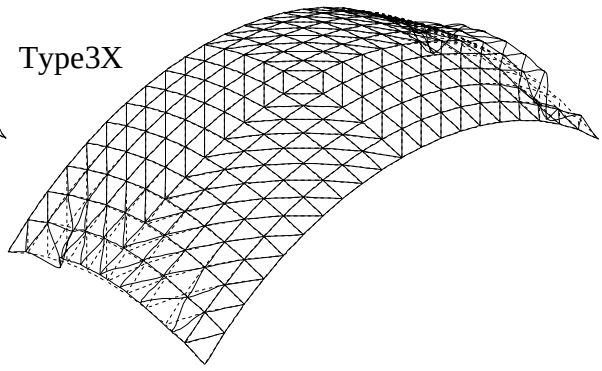

Fig. 10. Buckling Mode of Type3X.

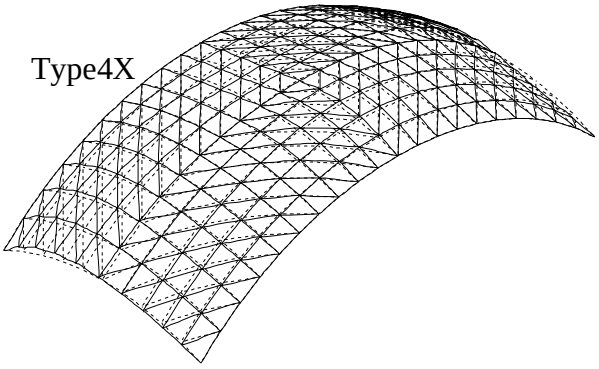

Fig. 11. Buckling Mode of Type4X.

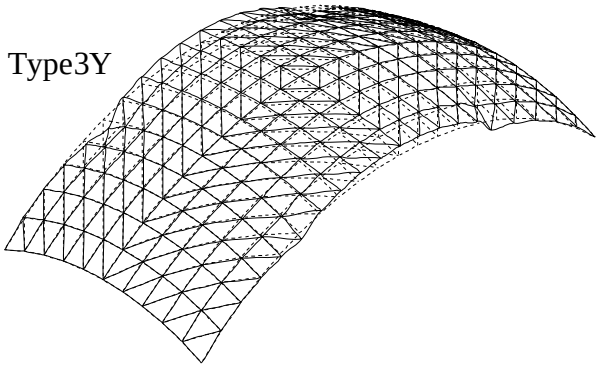

Fig. 12. Buckling Mode of Type3Y.

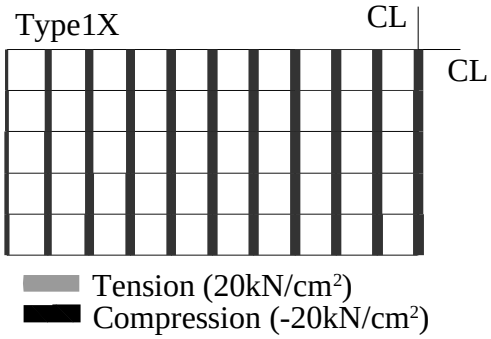

Fig. 13. Axial Stress Distribution of Type1X.

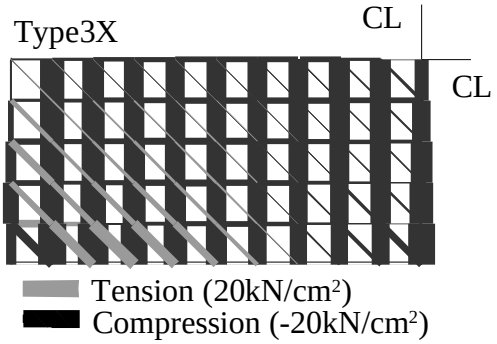

Fig. 14. Axial Stress Distribution of Type3X.

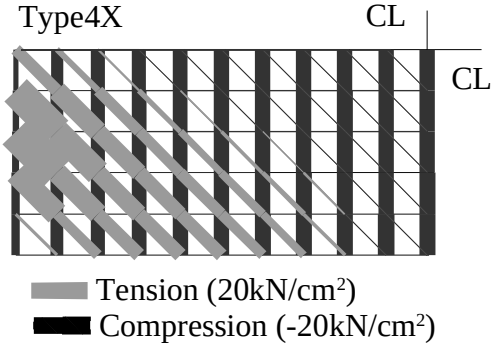

Fig. 15. Axial Stress Distribution of Type4X.

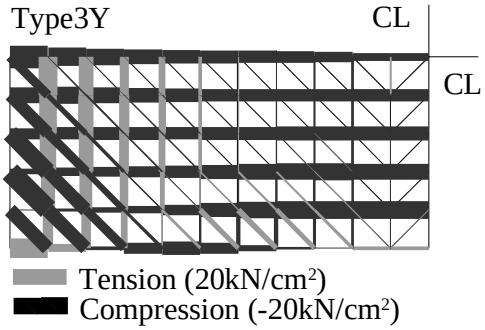

Fig. 16. Axial Stress Distribution of Type3Y.

3.4 Considerations

3.4.1 Buckling Load

The buckling load of Type1 using the new rigid joint is about 45 % smaller than that of Type2 using the perfect rigid joint. This shows that the degree of the new joint rigidity is almost proportional to the ratio of sectional property of sleeve to that of circular tube.

The ratio of the buckling load of Type1X to that of Type1Y is about 4. This value corresponds to the ratio of the buckling load of center arch of Type1X to that of Type1Y. This shows that the buckling load of orthogonal two-way grid shell in case of boundary condition treated here reflects the characteristic of the arch.

The ratio of the buckling load of Type3X to that of Type1X and the ratio of the buckling load of Type3Y to that of Type1Y are 2.49 and 6.07 respectively. This shows that the effect of the diagonal member on buckling load in case of peripheral nodes in Y direction being pin-supported is larger than that in case of peripheral nodes in X direction being pin-supported.

For the Type4 using PC bars as diagonal member to increase the buckling load, the ratio of buckling load of Type4X to that of Type1X and the ratio of buckling load of Type4Y to that of Type1Y are 1.55 and 1.14 respectively. This shows that in case of the location of PC bars

in this study, the effect of PC bars on the buckling load is influenced by the stress distribution of grid shell.

3.4.2 Buckling Mode

The buckling mode of Type1X and Type2X is a half wave in X direction and a full wave in Y direction. The buckling mode of Type3X is five half waves in Y direction at both free edges. The buckling mode of Type4X using PC bars as diagonal member is a full wave in both directions.

While peripheral nodes in Y direction are pin-supported, the buckling mode of Type3Y is three half waves in X direction and other model is a full wavelength in X direction. The effect of PC bar on the buckling mode is not distinct for the model in this boundary condition.

4. Conclusions

This paper treated the newly developed standardized truss system joint in order to apply to single layer two-way grid shell. The structural properties of this joint were determined by the bending experiment of joint. Then the buckling behaviors of grid shell using this joint system were calculated by the discrete numerical method. The efficiency of new rigid joint and the effect of PC bars used as the diagonal member on the buckling load and buckling mode of grid shell were discussed.

The following conclusions were drawn.

1) The relation of moment to rotational angle of this joint is almost approximated to tri-linear. The second slope appears at the separation of contact surfaces between the sleeve and the node and the third slope appears at yielding of bolt.

2) The separation moment of contact surfaces and yielding moment of joint increases as the member axial force changes from tension to compression.

3) From the comparison between the buckling load of the model using the new rigid joint and that of the model using the perfect rigid joint, the degree of the new joint rigidity is almost dependent on the ratio of sectional property of joint to that of circular tube.

4) The effect of PC bars on the buckling load is influenced by the stress distribution of grid shell in case of the location of PC bars in this study.

References

1. Imai K, Wakiyama K, Tsujioka S and Yamada Y : Proposing a New Joint System (KT-system) of Space Frame with Threaded Spherical Nodes and its Fatigue Characteristics, Int. Conf. IASS, Madrid Spain, Vol. 4, 1989

2. Taniguchi Y, Saka T and Shuku Y : Buckling Behaviour of Space Trusses Constructed by a Bolted Jointing System, Proc. 4th International Conference on Space Structures, Guildford, 1993, pp. 89-98

3. Tsujioka S, Yamada Y, Yasui N, Imai K and Wakiyama K : Fatigue Properties of Joint System with Threaded Spherical Nodes, J. Struct. Constr. Eng. AIJ, No. 490, Dec., 1996, pp. 223-228

4. Nooshin H, Disney P and Yamamoto C : Formian, Multi-Science Pub., 1993

5. Fujimoto M, Saka T, Imai K and Morita T : Experimental and Numerical Analysis of Buckling of a Single-layer Latticed Dome, Proc. 4th International Conference on Space Structures, Guildford, 1993, pp. 396-405